DOI: 10.1002/anie.200803383

Mesocrystals

Calcite Crystals with Platonic Shapes and Minimal Surfaces**

Rui-Qi Song, An-Wu Xu, Markus Antonietti, and Helmut Cölfen**

Platonic solids[1] are the five polyhedrons with equivalent facets composed of congruent convex regular polygons, in which the same number of facets meet at every vertex. The octahedron, with eight facets, is a platonic shape composed of triangles, and the dodecahedron, with 12 facets, is the only one with pentagonal facets. In nature, pyrite frequently occurs as octahedral or dodecahedral crystals. Certain viruses and radiolaria also routinely take the form of these regular polyhedral shapes.[2] A number of synthetic inorganic crystals with platonic shapes have been reported recently, such as gold nanocrystals,[3a] mesoporous silicate dodecahedra and octahedra,[3b,c] SnO_2 octahedra,[3d] In_2O_3 and Cu_2O octahedra,[3e,f] as well as metallic alloy quasi-crystals.[3g–i] For the trigonal $CaCO_3$ calcite crystal structure, the formation of platonic shapes is, owing to a too-low symmetry, not to be expected. Calcite pseudo-dodecahedra, nevertheless, were synthesized with a variety of additives, such as Mg^{2+},[4a–c] Co^{2+},[4d] simple organic acids,[4e] phosphate,[4f] carboxylate-rich polymers,[4g] amino acids,[4h] calcite-binding helical peptide,[4i] globular proteins,[4j] protein extracts isolated from aragonitic abalone shell nacre[4k] and from sea urchins.[4l,m] The mechanisms of crystal growth of these calcite pseudo-dodecahdra are additive adsorption on the {011} faces,[4l,n] the inhibiting effect of additives on step-growth,[4c] or the combination of the two functions.[4] Calcite mesocrystals with pseudo-octahedral morphology[5a,b] and otoconia-like morphology[5c] were also described.

However, a unified route towards more than one platonic calcite shape based on one same mechanistic approach has not yet been revealed. Herein, we present a nonclassical crystallization approach towards calcite with a platonic shape based on nanoparticle aggregation. We show that a commercial co-polyelectrolyte can be used to manoeuvre the crystallization of $CaCO_3$ into *meso*-crystalline calcite structures with curved surfaces and platonic shapes. Significantly, the intermediates are consistent with rhombohedral primitive (P)-surface morphology (see Supporting Information Figure S1)—one of the mathematical minimal surfaces, which were found in nature and in synthetic bicontinuous mesophases.[6a,b,7] The most striking example is the skeleton of *Cidaris rugosa*, in which self-assembled 3D networks have a continuous curvature. The importance of the P-surface structure was also recognized in other sea-urchin skeletal plates and has been connected with their functions in nutrient permeation, stress distribution, and their unique optical properties.[6,8]

The platonic calcite crystals were generated by a simple gas-diffusion method[9] in the presence of poly(4-styrenesulfonate-*co*-maleic acid) (PSS-*co*-MA). This polymer was chosen as it combines the maleic acid, which stabilizes {011} faces of calcite,[4e] with the mesocrystal-inducing properties of PSS[10] in one molecule. Pseudo-dodecahedral crystals were obtained for a polymer concentration of $0.1\ g\,L^{-1}$ and $[CaCl_2] = 1.25$ mM after 2 weeks crystallization. Figure 1a and Figure 1b show the typical scanning electron microscopy (SEM) images of the pseudo-dodecahedral calcite microcrystals obtained. It can be seen that exclusively pseudo-dodecahedral shapes were observed, with a relatively monodisperse size of approximately 20–30 μm. The transmission electron microscopy (TEM) image of an ultrathin section of the as-synthesized product (Supporting Information Figure S2) shows a remarkable large number of interstices within the bulk. The interstices suggest a crystallization

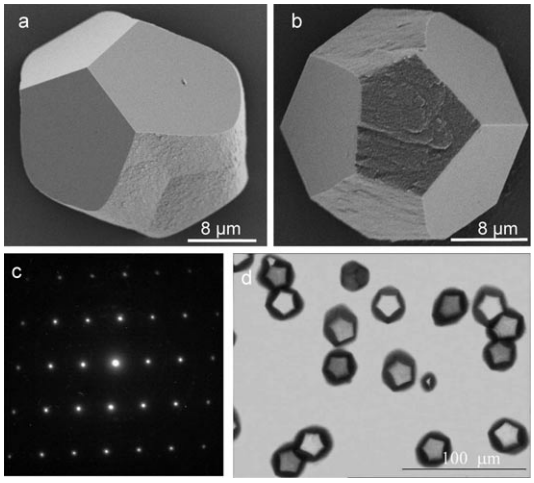

Figure 1. a, b) SEM images and d) optical microscopy of the pseudo-dodecahedral calcite crystals grown for two weeks. c) SAED pattern taken from an ultrathin section of the sample. [PSS-*co*-MA] = $0.1\ g\,L^{-1}$, $[CaCl_2] = 1.25$ mM.

[*] Dr. R.-Q. Song, Prof. Dr. M. Antonietti, Dr. H. Cölfen
Max Planck Institute of Colloids and Interfaces
Research Campus Golm, 14424 Potsdam (Germany)
Fax: (+49) 331-567-9502
E-mail: coelfen@mpikg.mpg.de
Prof. Dr. A.-W. Xu
Division of Nanomaterials and Chemistry, Hefei National Laboratory for Physical Sciences at Microscale, University of Science and Technology of China
Hefei 230026 (P.R. China)
Fax: (+86) 551-360-3040
E-mail: anwuxu@ustc.edu.cn

[**] We acknowledge the Max Planck Society for funding and thank Rona Pitschke for TEM characterization, Anne Heilig for AFM characterization, Denis Gebauer and Andreas Verch for titration measurement. This work was partially supported by the National Natural Science Foundation of China (20671096).

Supporting information for this article is available on the WWW under http://dx.doi.org/10.1002/anie.200803383.

pathway based on the aggregation of nanoparticles[11] and the presence of incorporated organic matter between the boundaries of the nanocrystallite domains. This feature was confirmed by thermal gravimetric analysis (TGA, not shown) which indicated a polymer content of approximately 2.2 wt%. The calcite polymorph was confirmed by X-ray diffraction (XRD) measurements (Supporting Information Figure S3a), in which the narrow peaks indicate a large coherence length, similar to reference calcite single crystals (Supporting Information Figure S3c). Selected-area electron diffraction (SAED) of the same sample shows single crystalline diffraction behavior indicating the high crystallographic orientation of the nanoparticles within the texture (Figure 1c). The pseudo-dodecahedral microstructure in solution is also nicely seen by optical microscopy (Figure 1d).

Looking more carefully at these structures, it is found that there are six smooth and six coarsened facets per pseudo-dodecahedron. We ascribe the smooth facets to the {104} family, these being the usually exposed faces of calcite, whereas the coarse facets do not look like real faces at all, as they seem to have curvature and blips with a typical nanogranular surface structure (Figure S4; Supporting Information).

In principle, those six rough faces could be indexed as {011}, an assignment supported by Cerius^2 modeling (Figure S5; Supporting Information). However, the curved and buckled appearance, the absence of evidence for step-growth (Figure 1a and Supporting Information Figure S4), as well as the neutral character of the {011} faces (which means they should not interact with the polyanion) call for a different interpretation.

Crystallization of $CaCO_3$ in 5 mM $CaCl_2$ solution with PSS-*co*-MA as an additive at a concentration of 0.1–0.25 g L^{-1} led to a similarly puzzling observation; the formation of pseudo-octahedral calcite superstructures (accompanied by some transient, spherical vaterite particles which occur as a minor side product), as shown in Figure 2.

The pseudo-octahedral particles are also uniform, with a size of several tens of micrometers. In contrast to the pseudo-dodecahedral crystals, all the surfaces of the octahedral crystals are rough and curved. Although angles and edges on a larger scale are clearly rather well kept, it is clear that the exposed faces are not flat and do not belong to the natural faces of calcite. Thus the system is forced to assemble these faces from differently oriented subunits.

A possible construction principle is revealed by light-microscopy observations. For some appropriately oriented particles, a three-fold symmetry is evident through the two opposite equilateral triangular facets per octahedral particle. We assign these two facets to (001) and (00−1), as evidenced by the absence of birefringence under crossed polarizers (Figure S6, Supporting Information).[5b,12] The other remaining lateral triangular facets cannot be constructed by simple natural faces. Using faces of the {011} family for this interconnection would result in a trigonally deformed superstructure (Figure S7, Supporting Information): A real octahedron cannot be constructed from a calcite single crystal.

Minor amounts of pseudo-cuboctahedral calcite mesocrystals (Figure 3) reveal parts of the construction principle. The pseudo-cuboctahedra are clearly just truncated octahedrons, with the six truncation sites being smooth and ascribed to the {104} family. The eight octahedral faces are still curved to the inside, indicating that those directions are not exposed because of crystal symmetry, but are the result of a minimization of surface energy. This situation suggests the occurrence of a mesoscale transformation process: the aggregates are not single crystals, but energy-minimized superstructures of nanocrystals. It should be noted that both the texture and size of the pseudo-octahedral calcite microcrystals are different from those of the pseudo-octahedral calcite mesocrystal morphologies constructed from rhombohedral building units in polyacrylamide gels.[5,12c] While a hierarchical aggregation of rhombohedral subunits is discussed for the gel case,[5,12c] our pseudo-octahedral mesocrystals synthesized in solution clearly show facetted faces indicative of a single crystal as well as curved surfaces indicative of minimal surfaces (Figure 2 and Figure 3).

Aggregation of nanocrystalline calcite subunits results again in the occlusion of polymers in the pseudo-octahedra. TGA investigation (data not shown) showed a polymer content of approximately 4 wt% in the final product, higher than in the pseudo-dodecahedra. TEM was employed to

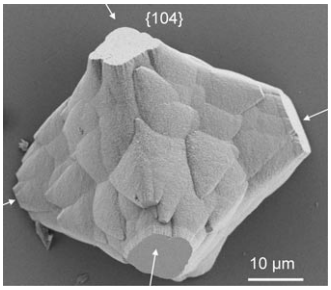

Figure 3. SEM image of the pseudo-cuboctahedral morphology of calcite aggregates. Six smooth faces (six apexes of the truncated octahedron) are ascribed to the {104} family, as indicated by arrows. [PSS-*co*-MA] = 0.1 g L^{-1}, [$CaCl_2$] = 5 mM, 2 weeks.

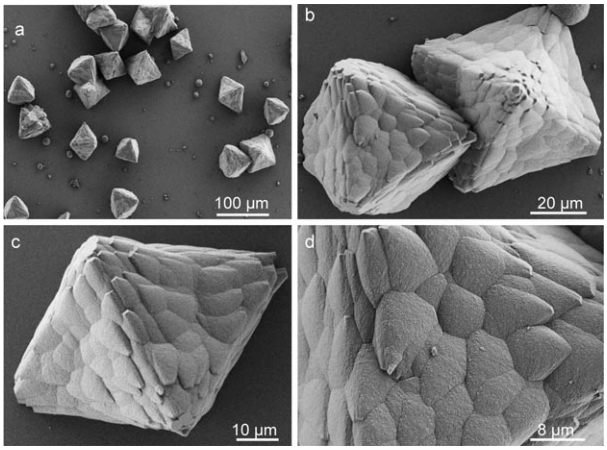

Figure 2. SEM images of pseudo-octahedral calcite mesocrystals grown for two weeks. [PSS-*co*-MA] = 0.1–0.25 g L^{-1}, [$CaCl_2$] = 5 mM.

observe the microstructure of the pseudo-octahedral particles. TEM images of an ultrathin section of the octahedral calcite mesocrystals (Figure S8, Supporting Information) show that the sample has a mesoporous structure, which originates from the interstitial voids of the packed primary nanoparticles. The nanoparticles, size of approximately 20–50 nm, are slightly smaller than the calcite building units in the final crystals (Figure S3b, Supporting Information).

Mesopores and defects under preservation of a collective crystal orientation are important characteristics of mesocrystals.[10,11,13] SAED (the inset in Figure S8b, Supporting Information) shows a single-crystal diffraction pattern with minor distortions. Although individual nanoparticles within a local area seem to be non-oriented, the overall aggregate still exhibits the same lattice fringe orientation, indicating the long-range ordering of most nanocrystallites through vectorial aggregation.[11,14] Further, the octahedral calcite has a BET surface area of 64.8 $m^2 g^{-1}$, which is much larger than the BET surface area (1.8 $m^2 g^{-1}$) of calcite grown in the absence of polymer. In addition, the wide-angle X-ray scattering (WAXS) peaks (Figure S3, Supporting Information) are broadened, and the primary particle size is determined to be 60–70 nm.

To identify the underlying mechanisms, we performed time-resolved experiments. SEM (Figure 4), TEM, and SAED (Figure S9, Supporting Information) of the precursors indicate a large number of amorphous $CaCO_3$ nanoparticles as first species, indicating nucleation inhibition by PSS-*co*-MA (Figure S10, Supporting Information). These nanoparticles form an unstructured aggregate (Figure 4), which then develops crystalline form and facets.

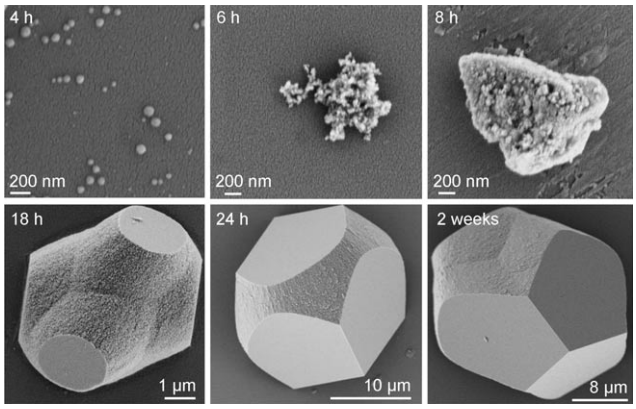

Figure 4. SEM images of precursor and intermediates obtained by time-resolved experiments. [Polymer] = 0.1 $g L^{-1}$, [Ca^{2+}] = 1.25 mM.

Figure 5 shows two intermediates of pseudo-dodecahedra derived from time-dependent experiments performed with different Ca^{2+} ion and polymer concentrations. Strikingly, all the SEM images of these intermediates suggest a rhombohedral P-surface morphology[7] made up by nanoparticles. Typically, minimal surfaces on the micro- and macroscale occur only for liquid phases with surface tension, such as lipid–water or surfactant–water mixtures[6a] as well as copolymers and liquid-crystalline mesophases of amphiphiles in

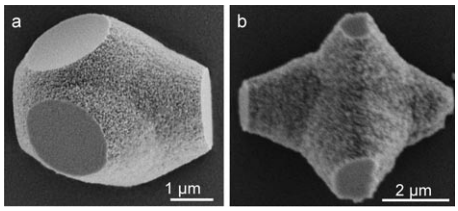

Figure 5. SEM image of intermediates of the pseudo-dodecahedral structure grown after a) 18 h, [PSS-*co*-MA] = 0.1 $g L^{-1}$, [$CaCl_2$] = 1.25 mM, b) 3 days, [PSS-*co*-MA] = 0.0025 $g L^{-1}$, [$CaCl_2$] = 1.25 mM.

water. On the scale of atoms to a few crystal unit cells, minimal surfaces were also reported for zeolites[6b] and equipotential lines in crystal grids.[6c]

We assume that the inorganic particles and PSS-*co*-MA form a joint liquid–solid phase, stabilized by hydrogen-bond formation[15] and the strong calcium-binding ability of the polymer (Figure S10, Supporting Information). The steric stabilization of the primary particles by the polymer competing with the van der Waals attraction then allows formation of a soft-condensed phase, which also provides the primary nanoparticle aggregates with a moderate degree mobility that enables them to regulate their mutual positions in the oriented aggregate.[16]

In classical crystallization, the shape of crystals grown in solution is thermodynamically defined by minimizing the interface energies and the surface area of all the exposed faces (Wulffs rule).[17] This rule clearly undergoes a generalization when nanocrystal assemblies or mesocrystals are involved, including the formation of minimal surfaces in the intermediates of the pseudo-dodecahedral and curved faces in the pseudo-octahedral crystals (see also Figure 1 and Figure 2) Such minimal surfaces are otherwise only known on the micro- and macroscale from lipid bilayers, copolymers, and liquid-crystalline mesophases of amphiphiles. The mesocrystals in Figure 2 therefore behave like a crystalline solid and a liquid at the same time. The "hard", weakly polymer-controlled crystallization directions typical for a single crystal define directionality and number of crystalline edges, whereas the polymer-stabilized, hydrated, "soft directions" show features of a liquid and are determined by the joint liquid-like character and its surface tension. This combination enables the generation of rounded surfaces and the exposure of directions which are not elements of the primary crystal symmetry.

We highlight that P-surface intermediates are energetically metastable structures with minimized surface area. The six plain {104} faces of the crystal superstructure on the tip of the pseudo-octahedra just grow in size (Figure 4), and the remaining six rough faces are energy-minimized surfaces connecting the predefined corners as in a liquid, adopting minimal and curved surfaces. This process is seen throughout the structural development of the pseudo-dodecahedra in Figure 4.

The overall orientation in a densely packed superstructure simplifies recrystallization towards a fused crystal, as was observed for some mesocrystals by small-angle neutron

scattering (SANS) measurements.[18] That such a transformation might also occur for the mesocrystals presented herein is indicated by the cuboctahedrons, in which the {104} faces have clearly been recrystallized and smoothened by Ostwald ripening.

In summary, calcite superstructures with two different platonic shapes have been synthesized by a simple and unified method of polymer-controlled crystallization. Intriguingly, the shape transition can be easily manipulated through regulation of the reaction conditions with a single polymer additive. The expression of platonic morphologies is the result of a cooperative assembly process of primary nanocrystals and mesocrystal formation, where attraction energy and surface-area minimization drive the formation of the intermediate and final structures, which contain elements of the behavior of both crystals as well as liquids. This finding for a synthetic crystallization system might help to explain several observations of naturally formed biomineral structures in which minimal surfaces are exposed.

Experimental Section

All chemicals—calcium chloride, and ammonium carbonate (Aldrich), poly(4-styrenesulfonate-*co*-maleic acid) (PSS-*co*-MA; sodium salt, 25 wt% in water, obtained from Aldrich, average molecular weight = 20000 g mol^{-1}, styrene sulfonate/maleic acid molar ratio = 3:1)—were of analytical grade and were used without further purification. All glassware (glass bottle and small pieces of glass substrate) was cleaned and sonicated in ethanol for 5 min, rinsed with distilled water, and further soaked with an H_2O/HNO_3 (65%)/H_2O_2 (1:1:1 V/V/V) solution, then rinsed with doubly distilled water, and finally dried in air with acetone.

The crystallization of $CaCO_3$ was carried out in a closed desiccator at room temperature (22 ± 3 °C). In a typical run, a solution (A) of $CaCl_2$ (20 mM) and a mixture solution (B) containing polymer (12.5 g L^{-1}) and $CaCl_2$ (20 mM) were prepared by using doubly distilled water through which nitrogen had been bubbled overnight. After solution A (9.8 mL) and solution B (0.2 mL) were injected into a glass bottle (30 mL) with glass slides at the bottom, and stirred, the bottle was covered with parafilm, punched with three holes, and placed in a closed desiccator at room temperature. Prior to this a glass beaker (50 mL) with crushed ammonium carbonate powder was also covered with Parafilm, punched with three needle holes and put at the bottom of the desiccator. After 2 weeks, the crystals were recovered, briefly washed with water, and allowed to dry. After gold coating, the crystals were examined with a scanning electron microscope. Powder X-ray diffraction (XRD) patterns were recorded on a PDS 120 diffractometer (Nonius GmbH, Solingen) with $Cu_{K\alpha}$ radiation ($\lambda = 1.542$ Å).

Thermogravimetric analysis was carried out under a stream of nitrogen, at a heating rate of 10 °C min^{-1} using a Netzsch TGA-209. N_2 adsorption measurements were performed at 77 K using a Micromeritics ASAP 2010 system utilizing Barrett–Emmett–Teller (BET) calculations for surface area and Barrett-Joyner-Halenda (BJH) calculations for pore size distribution for the adsorption branch of the isotherm. The SEM measurements were performed on a LEO 1550 GEMINI microscope. TEM, HRTEM images, and SAED were obtained on a JEOL 2010 microscope operated at 200 kV. The samples were embedded in epoxy resin and ultramicrotomed for the TEM measurements. The surface cleavage of the crystal faces, the unit cell structure, and the modeling of morphology were performed with the Cerius^2 software (Accelrys). WAXS patterns were simulated with the MS-Modelling Software (Accelrys). The AFM images were obtained by means of a Digital Instruments nanoscope IIIa Multimode AFM (Digital Instruments Inc., Santa Barbara, CA).

Received: July 11, 2008
Published online: December 9, 2008

Keywords: bio-inspired mineralization · calcium · crystal growth · minimal surfaces · solid-state structures

[1] a) H. S. M. Coxeter, *Regular Polytopes*, Dover Publications, New York, **1973**; b) D. M. Davis, *The Nature and Power of Mathematics*, Princeton University Press, Princeton, **1993**.

[2] A. J. Levine, *Viruses*, Scientific American Library, New York, **1991**.

[3] a) F. Kim, S. Connor, H. Song, T. Kuykendall, P. D. Yang, *Angew. Chem.* **2004**, *116*, 3759 – 3763; *Angew. Chem. Int. Ed.* **2004**, *43*, 3673 – 3677; b) C. Yu, B. Tian, J. Fan, G. D. Stucky, D. Zhao, *J. Am. Chem. Soc.* **2002**, *124*, 4556 – 4557; c) H. J. lee, Y. M. Kim, O. S. Kweon, I. J. Kim, *J. Eur. Ceram. Soc.* **2007**, *27*, 561 – 564; d) H. G. Yang, H. C. Zeng, *Angew. Chem.* **2004**, *116*, 6056 – 6059; *Angew. Chem. Int. Ed.* **2004**, *43*, 5930 – 5933; e) Y. F. Hao, G. W. Meng, C. H. Ye, L. D. Zhang, *Cryst. Growth Des.* **2005**, *5*, 1617 – 1621; f) B. Deng, A. W. Xu, G. Y. Chen, R. Q. Song, L. P. Chen, *J. Phys. Chem. B* **2006**, *110*, 11711 – 11716; g) W. Ohashi, F. Spaepen, *Nature* **1987**, *330*, 555 – 556; h) H. Hubert, B. Devouard, L. A. J. Garvie, M. O'Keeffe, P. R. Buseck, W. T. Petuskey, P. F. McMillan, *Nature* **1998**, *391*, 376 – 378; i) A. P. Tsai, *Acc. Chem. Res.* **2003**, *36*, 31 – 38.

[4] a) S. Albeck, J. Aizenberg, L. Addadi, S. Weiner, *J. Am. Chem. Soc.* **1993**, *115*, 11691 – 11697; b) S. Raz, S. Weiner, L. Addadi, *Adv. Mater.* **2000**, *12*, 38 – 42; c) K. J. Davis, P. M. Dove, J. J. De Yoreo, *Science* **2000**, *290*, 1134 – 1137; d) A. L. Braybrook, B. R. Heywood, R. A. Jackson, K. Pitt, *J. Cryst. Growth* **2002**, *243*, 336 – 344; e) S. Mann, D. D. Archibald, J. M. Didymus, T. Douglas, B. R. Heywood, F. C. Meldrum, N. J. Reeves, *Science* **1993**, *261*, 1286 – 1292; f) J. M. Didymus, P. Oliver, S. Mann, A. L. Devries, P. V. Hauschka, P. Westbroek, *J. Chem. Soc. Faraday Trans.* **1993**, *89*, 2891 – 2900; g) S. B. Mukkamala, C. E. Anson, A. K. Powell, *J. Inorg. Biochem.* **2006**, *100*, 1128 – 1138; h) C. A. Orme, A. Noy, A. Wierzbickl, M. T. McBride, M. Grantham, H. H. Teng, P. M. Dove, J. J. DeYoreo, *Nature* **2001**, *411*, 775 – 779; i) D. B. DeOliveria, R. A. Laursen, *J. Am. Chem. Soc.* **1997**, *119*, 10627 – 10631; j) A. Hernández-Hernández, A. B. Rodríguez-Navarro, J. Gómez-Morales, C. Jiménez-Lopez, Y. Nys, J. M. García-Ruiz, *Cryst. Growth Des.* **2008**, *8*, 1495 – 1502; k) G. Fu, S. Valiyaveettil, B. Wopenka, D. E. Morse, *Biomacromolecules* **2005**, *6*, 1289 – 1298; l) S. Albeck, S. Weiner, L. Addadi, *Chem. Eur. J.* **1996**, *2*, 278 – 284; m) C. R. Mackenzie, S. M. Wilbanks, K. M. McGrath, *J. Mater. Chem.* **2004**, *14*, 1238 – 1244; n) S. Mann, *Nature* **1993**, *365*, 499 – 505; o) J. J. De Yoreo, P. M. Dove, *Science* **2004**, *306*, 1301 – 1302.

[5] a) O. Grassmann, G. Muller, P. Löbmann, *Chem. Mater.* **2002**, *14*, 4530 – 4535; b) O. Grassmann, P. Löbmann, *Chem. Eur. J.* **2003**, *9*, 1310 – 1316; c) Y. X. Huang, J. Buder, R. Cardos-Gil, Y. Prots, W. Carrillo-Cabrera, P. Simon, R. Kniep, *Angew. Chem.* **2008**, *120*, 8404 – 8408; *Angew. Chem. Int. Ed.* **2008**, *47*, 8280 – 8284.

[6] a) S. T. Hyde, S. Andersson, K. Larsson, Z. Blum, T. Landh, S. Lidin, B. W. Ninham, *The Language of Shape*, Elsevier, Amsterdam, **1997**; b) B. Chen, M. Eddaoudi, S. T. Hyde, M. O'Keeffe, O. M. Yaghi, *Science* **2001**, *291*, 1021 – 1023; c) R. Nesper, H. G. von Schnering, *Angew. Chem.* **1986**, *98*, 111 – 113; *Angew. Chem. Int. Ed. Engl.* **1986**, *25*, 110 – 112.

[7] G. E. Schröder, S. J. Ramsden, A. Fogden, S. T. Hyde, *Phys. A* **2004**, *339*, 137 – 144.

[8] a) H. U. Nissen, *Science* **1969**, *166*, 1150 – 1152; b) M. Lai, A. N. Kulak, D. Law, Z. B. Zhang, F. C. Meldrum, D. J. Riley, *Chem.*

Commun. **2007**, 3547 – 3549; c) Y. H. Ha, R. A. Varia, W. F. Lynn, J. P. Costantino, J. Shin, A. B. Smith, P. T. Matsudaira, E. L. Thomas, *Adv. Mater.* **2004**, *16*, 1091 – 1094.
[9] A. N. Kulak, P. Iddon, Y. Li, S. P. Armes, H. Cölfen, O. Paris, R. M. Wilson, F. C. Meldrum, *J. Am. Chem. Soc.* **2007**, *129*, 3729 – 3736.
[10] a) T. X. Wang, H. Cölfen, M. Antonietti, *J. Am. Chem. Soc.* **2005**, *127*, 3246 – 3247; b) T. X. Wang, H. Cölfen, M. Antonietti, *Chem. Eur. J.* **2006**, *12*, 5722 – 5730.
[11] H. Cölfen, M. Antonietti, *Angew. Chem.* **2005**, *117*, 5714 – 5730; *Angew. Chem. Int. Ed.* **2005**, *44*, 5576 – 5591.
[12] a) H. Imai, T. Terada, S. Yamabi, *Chem. Commun.* **2003**, 484 – 485; b) C. R. MacKenzie, S. M. Wilbanks, K. M. McGrath, *J. Mater. Chem.* **2004**, *14*, 1238 – 1244; c) O. Grassmann, R. B. Neder, A. Putnis, P. Löbmann, *Am. Mineral.* **2003**, *88*, 647 – 652.
[13] A. W. Xu, M. Antonietti, S. H. Yu, H. Cölfen, *Adv. Mater.* **2008**, *20*, 1333 – 1338.
[14] H. Cölfen, M. Antonietti, *Mesocrystals and Nonclassical Crystallization*, Wiley, Hoboken, **2008**.
[15] E. Tjipto, J. F. Quinn, F. Caruso, *Langmuir* **2005**, *21*, 8785 – 8792.
[16] a) A. P. Alivisatos, *Science* **2000**, *289*, 736 – 737; b) J. F. Banfield, S. A. Welch, H. Zhang, T. T. Ebert, R. L. Penn, *Science* **2000**, *289*, 751 – 754.
[17] G. Wulff, *Z. Kristallogr.* **1901**, *34*, 449 – 530.
[18] D. Schwahn, Y. R. Ma, H. Cölfen, *J. Phys. Chem. C* **2007**, *111*, 3224 – 3227.

